2021 43rd Annual International Conference of the
IEEE Engineering in Medicine & Biology Society (EMBC)
Oct 31 - Nov 4, 2021. Virtual Conference

Applicability of Narrow Groove Theory in Designing Washout Features for Rotary Blood Pumps*

Shelby A. Bieritz, P. Alex Smith, Yaxin Wang, William E. Cohn, Jane Grande-Allen

Abstract— **High and low shear regions in rotary blood pumps require sufficient washout flow to minimize blood residence time, thereby preventing hemolysis or regions of stasis that can lead to pump thrombosis. Spiral groove bearings (SGBs) both enhance pump washout and reduce erythrocyte exposure to high shear. Narrow groove theory (NGT) has been used as an analytical tool to estimate the flow performance of a flat SGB during the design stage. However, NGT cannot accurately predict the performance of a conical SGB. In this study, we formulated an analytical model from the established NGT by adding an inertia correction term to incorporate variations in centrifugal force, which improved washout prediction in a conical SGB. The modified NGT model was then validated by comparison with experimental results. The results show that the modified NFT analytical model can reasonably predict washout rate when the spiral groove geometry favors creep flow conditions. The conical half angle of the SGB had the most significant impact on washout, with a decrease in half angle leading to large increases in washout flow. Small half angles also maintained viscous pumping at larger Reynolds numbers. In summary, the modified NGT can be a useful tool for designing conical SGBs for rotary blood pump washout within the creep flow regime.**

I. Introduction

Spiral grooves are typically machined or etched onto a rotor surface to provide hydrodynamic bearing stiffness to rotating components. As they rotate, the spiral grooves pump fluid along the length of the narrowing groove, building pressure in the fluid film while generating an inward flow in the bearing gap [1, 2]. Thus, spiral groove bearings (SGBs) intrinsically act as hydrodynamic bearings and viscous pumps, and flat SGBs have demonstrated utility in promoting blood flow (washout) while assuming a load-bearing role in centrifugal blood pumps [3-6]. Pump washout prevents extended blood exposure to high shear rates for an extended period of time, causing hemolysis and platelet activation and increasing the severity of sub-lethal red blood cell damage [7-10]. Regions of stasis also lead to thrombus formation, which can cause pump failure and high mortality rates [11-14]. In addition to improving washout, SGBs are hypothesized to protect red blood cells from high shear rates in the bearing gap by entraining cells in the bearing grooves; this has been visually demonstrated at a 1% hematocrit [15-17]. Based on their washout and erythrocyte protection capacity, SGBs may improve RBP safety.

The load-bearing capacity of SGBs was first characterized by Muijderman in an analytical model termed narrow groove theory (NGT) [1, 2]. From the Navier-Stokes equations, Muijderman derived an expression for the radial pressure rise along the SGB surface and presented a special case for pressure rise in the presence of transverse leakage flow in a flat bearing gap. Bootsma expanded upon Muijderman's work by incorporating an unspecified leakage flow term into the pressure equations for both conical and spherical SGBs [18]. The NGT has been validated for predicting the load capacity of flat, spherical, and herringbone-grooved SGBs, both experimentally and computationally [2, 3, 18, 19]. One shortcoming of the NGT is that centrifugal forces acting on fluid in a flat bearing gap reduce load capacity measurements below theoretical predictions [2]. A correction to the load capacity equation to address centrifugal forces was then proposed but was found to be accurate only at low speeds where centrifugal forces were negligible.

The NGT has also been used to approximate SGB leakage. Kink and Reul resolved flow patterns in flat SGBs with a computational model and validated the NGT for approximating leakage in sealed SGBs for axial blood pumps [4]. Chan et al. addressed the effect of centrifugal forces on mass flow in an unsealed flat SGB gap with an inertia correction term that describes diminishing transverse flow as bearing gap increases [19]. Amaral et al. altered flat SGB geometry to maximize leakage flow and demonstrated agreement between experimental flow curves and the NGT with Chan's correction [3].

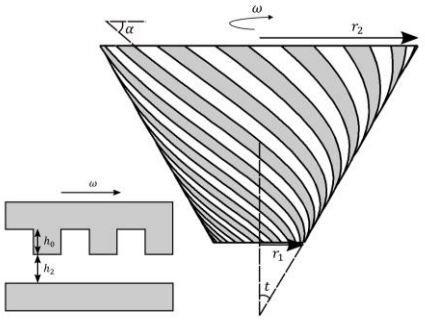

Figure 1. Diagram of a conical spiral groove bearing with geometry labeled. Subset shows the bearing gap with groove dimensions specified.

NGT applicability as a flow prediction tool has been limited to flat SGB geometries. Here, we have assessed the NGT for conical SGBs (Fig. 1) and introduced an empirical inertia correction term to improve flow approximation. We examined a conical SGB because of its ability to generate washout flow

* This work was supported in part by the U.S. National Science Foundation Graduate Research Fellowship under Grant No. 1450681 and by the Alexander Family Trust Fund.

Shelby A. Bieritz is with the Department of Bioengineering, Rice University, Houston, Texas, USA (e-mail: Shelby.A.Bieritz@rice.edu).

P. Alex Smith is with the Innovative Device and Engineering Applications, Texas Heart Institute, Houston, TX 77030 USA (e-mail: palexs@gmail.com).

Yaxin Wang is with the Innovative Device and Engineering Applications, Texas Heart Institute, Houston, TX 77030 USA (office: 832-355-5508; fax: 832-355-9552; e-mail: ywang@texasheart.org).

William E. Cohn was with the Center for Preclinical Surgical & Interventional Research, Texas Heart Institute, and now is with the Center for Device Innovation @ TMC, Johnson & Johnson, Houston, TX, USA (e-mail: wcohn@texasheart.org).

Jane Grande-Allen is with the Department of Bioengineering, Rice University, Houston, Texas, USA (e-mail: grande@rice.edu).

in an axial direction, which may be useful in promoting washout in miniature axial-flow ventricular assist devices. In addition, we have demonstrated the effects of groove geometry variations on flow generation through benchtop experiments. Finally, we discuss the limitations of the NGT as a leakage flow prediction tool for conical spiral groove geometries.

II. Methods

A. Analytical SGB Washout Model

To explore NGT accuracy for conical SGB washout, we first adapted Muijderman's equations describing the pressure and mass flow in a flat SGB gap to a conical surface. Nomenclature for the NGT is listed in Table 1.

The following system of equations was derived, starting with the equation for pressure rise in a flat SGB gap:

$$P = \frac{6\eta}{h^2}\int_{r2}^{r1} \omega r g_1 - \frac{S_t(1+\gamma)Y}{h_1 \pi r \rho} dr \quad (1)$$

where g_1 and Y are both geometric functions given below,

$$g_1 = \frac{\gamma H^2 \cot\alpha (1-H)(1-H^3)}{(1+\gamma H^3)(\gamma+H^3)+H^3\cot^2\alpha(1+\gamma)^2} \quad (2)$$

$$Y = \frac{H^2(1+\cot^2\alpha)(\gamma+H^3)}{(1+\gamma H^3)(\gamma+H^3)+H^3\cot^2\alpha\,(1+\gamma)^2} \quad (3)$$

Transforming this equation for a conical gap and integrating over the transverse bearing length gives

$$P(s) = \frac{6\eta\omega \sin(t)^2 g_1}{h^2}\frac{(s_2^2 - s^2)}{2} - \frac{6\eta S_t(1+\gamma)}{h^2 h_1 \pi \rho} Y ln\left(\frac{s_2}{s}\right) \quad (4)$$

To quantify the gap leakage in a flat bearing, Muijderman used (1) to solve the pressure rise over the ungrooved bearing surface from an arbitrary radius, r_b to r_1. The pressure equation becomes logarithmic, and the pressure at r_1 can be set to 0. The flow term can then be solved as a function of P_{r_b}. Similarly, the pressure rise along an ungrooved conical bearing surface can be solved between an arbitrary transverse length, s_b, and s_1, which gives

$$S_t = \frac{P_{s_b} h^3 \pi \rho}{6\eta(1+\gamma) ln\left(\frac{s_b}{s_1}\right)} \quad (5)$$

TABLE I. Nomenclature for the Narrow Groove Theory for Flat and Conical SGB Geometries

Symbol	Quantity
P	Pressure rise over transverse bearing surface
P^*	Modified pressure rise over transverse bearing surface
P_{s_b}	Pressure rise at an arbitrary transverse length
η	Dynamic viscosity
h	Gap between bearing ridges and mating journal surface
h_0	Groove depth
h_1	$h + h_0$
H	h/h_1
ω	Angular velocity
r	Spiral groove bearing radius (integration variable)
r_1	Inner spiral groove bearing radius
r_2	Outer spiral groove bearing radius
s	Transverse bearing distance from conical origin
s_1	Transverse bearing distance at r_1 of a conical spiral groove bearing
s_2	Transverse bearing distance at r_2 of a conical spiral groove bearing
s_b	Arbitrary transverse bearing length
S_t	Mass leakage flow rate through the bearing gap
t	Conical half angle
ρ	Fluid density
α	Groove angle
γ	Ridge width to groove width ratio

The pressure rise at the transverse length, P_{s_b}, is solved using (4) from P_{s_2} to P_{s_b}, substituting (5) for S_t, which solves the leakage flow in the bearing gap. Finally, the corrections for centrifugal forces were incorporated. To correct for inertial effects, we derived a term from Navier-Stokes equations in cylindrical coordinates. We reduced the inertial term to

$$-\int \frac{\rho U_\theta^2}{r} dr. \quad (7)$$

Amaral and Chan utilized (7) to correct the pressure rise for a flat bearing and found agreement with experimental data [3, 19]. Transforming the integral to the conical coordinate system and integrating, we can write the inertia term as

$$-\frac{1}{2}\rho\, sin(t)^2\, \omega^2 s_1^2 \quad (8)$$

This term was subtracted from the pressure term in (5) and (4) for the overall pressure rise along the conical surface, giving a modified pressure equation:

$$P^*(s) = P(s) - \frac{1}{2}\rho \sin(t)^2\, \omega^2 s_1^2 \quad (9)$$

Scaling bearing geometries up (5:1) enabled 3D printing of otherwise unprintably small features. Similitude estimated flow generation of the original-sized bearings from the scaled experiments. To accurately represent flow generated by an original-sized bearing in a blood pump, we matched the thin film Reynolds number (Equation 10) between scaled experiments and blood pump operating conditions, thus preserving the balance of inertial and viscous forces acting in the bearing gap. To match Reynolds number experimentally, we used 57wt% glycerol and reduced the operating speed from 20,000 to 1,940 rpm (Table 2). The nondimensionalized flow coefficient was then used to estimate original bearing flow generation from the scaled experimental data according to Equation 11, with β denoting the flow coefficient, Q the mass flow rate, ω the angular velocity, and h the bearing gap [20].

$$Re = \frac{\rho U h}{\mu} \quad (10)$$

$$\beta = \frac{Q}{\omega h^3} \quad (11)$$

TABLE II. Similitude Scaling of Miniature Conical SGB

	Kinematic viscosity (m^2/s)	OD (mm)	h_0 (μm)	rpm	Reynolds number
Original	3.01887E-06	7	60	20,000	126.8
Scaled	7.3232E-06	35	300	1,940	126.8

B. *Experimental Setup*

We prototyped (Objet30 Pro, Stratasys, USA) and tested (Fig. 2) the SGB designs. Bearings were driven by a motor (EC22, Maxon Motor, USA), wherein the x-y-z axes were independently controllable (Benchtop CNC Mill, MicroKinetics, USA). We measured x, y, and z bearing forces (Nano43 F/T Sensor, ATI Industrial Automation, USA). The bearings were centered radially and positioned with a 2 mm axial gap, then driven at a constant speed while decreasing the axial gap in 25-µm increments. The inflow and outflow of the bearing gap region were connected to a loop with a flow probe (BioProTT Clamp-On Transducer, em-tec, Germany). We varied 5 bearing parameters: groove depth, groove angle, ridge-to-groove width ratio, conical half angle, and rotational speed (Table 3). Each bearing was tested in triplicate. All theory calculations for comparison were completed in MATLAB R2016a (MathWorks, Natick, MA, USA). Statistics were analyzed in MATLAB using one-way ANOVA with post-hoc Tukey Honestly Significant Difference test. We calculated single-parameter correlations between geometry and performance using a Pearson correlation coefficient. All results were significant ($p<0.05$).

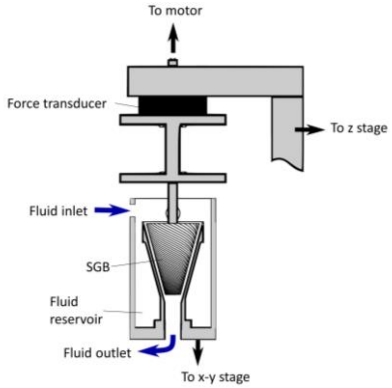

Figure 2. Spiral groove bearing (SGB) test rig to evaluate flow and force generation. The SGB was mounted to a motor and z-axis stage to adjust bearing gap. A mating journal surface in a fluid reservoir was mounted to an x-y stage for centering. Flow and force data were measured.

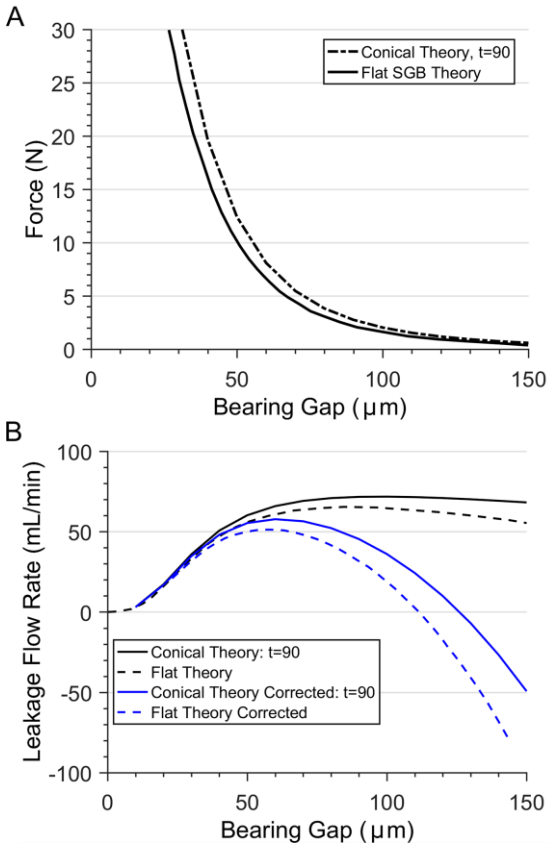

Figure 3. Calculated spiral groove bearing (SGB) force (a) and mass flow rate (b) using conical narrow groove theory are compared to previously reported calculations using the flat narrow groove theory [3]. A 90° half angle was used in the conical formulas, emulating a flat bearing. Calculations were performed with and without centrifugal force correction (8).

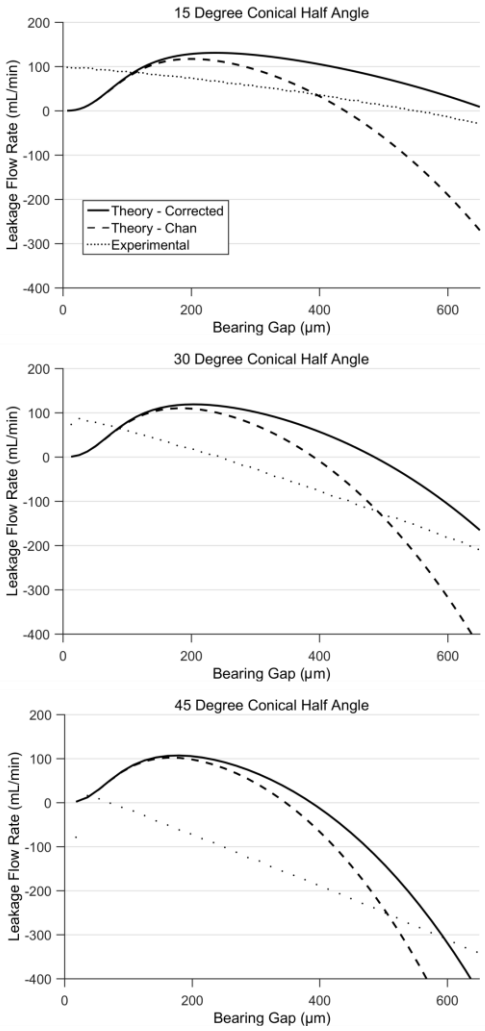

Figure 4. The narrow groove theory with inertial correction (11) is compared to Chan et al. [19] Conical spiral groove bearings (SGBs) with half angles 15°, 30°, and 45° were compared. The inertia correction proposed by Chan (Theory–Chan) was weighted by the sine squared of the conical half angle (Theory-Conical), which gives a more accurate approximation of leakage flow rate as the conical half angle is varied. The proposed correction also approaches Chan's correction for a flat SGB as the half angle increases.

TABLE III. BEARING DESIGNS TESTED EXPERIMENTALLY

	t (°)	h_0 (µm)	α (°)	rpm	γ
Baseline 1 (BL1)	15	300	27.5	1940	1
Variation from BL1	15	400, 500	22.5, 32.5	1450, 2425	2, 0.5
Baseline 2 (BL2)	30	300	25	1940	1

Variation from BL2	30	400, 500	20, 30	1450, 2425	2, 0.5
Half angle variation	45	300	22.5	1940	1

III. Results

A. Empirically Modified Analytical Model

The conical NGT was verified against the flat NGT calculations reported by Amaral et al. [3]. The conical pressure and mass flow rate equations were solved with a 90° conical half angle, equivalent to a flat SGB, and all other geometric inputs matched those reported by Amaral et al. (Fig. 3).

Fig. 4 shows that viscous pumping by conical SGBs was overcome by centrifugal forces as the bearing gap increased, demonstrated by a diminishing mass flow and flow reversal in the bearing gap. The gap at which flow reversal occurred was significantly correlated with the conical half angle (Pearson coefficient: -0.83, $p<0.001$). To reflect the dependence of flow reversal on the conical half angle, we proposed a modified inertia correction based on the study by Wimmer [21], who classified flow phenotype in a grooveless conical gap with a modified Froude number:

$$Fr = \frac{\omega^2 r \sin(\theta)}{g} \tag{10}$$

where g is gravitational acceleration, ω is the rotational speed, and r is the radius of the base of the cone. Weighting the Froude number with the sine of the half angle captured the balance of centrifugal and body forces in the conical gap.

In the conical SGB gap, the Reynolds number is more important than the Froude number, but since centrifugal forces are strongest in a flat bearing gap and weakest in a cylindrical gap, the correction in (8) was further weighted by the sine of the half angle squared, as this matched experimental results most closely (Fig. 4). The proposed correction is shown below:

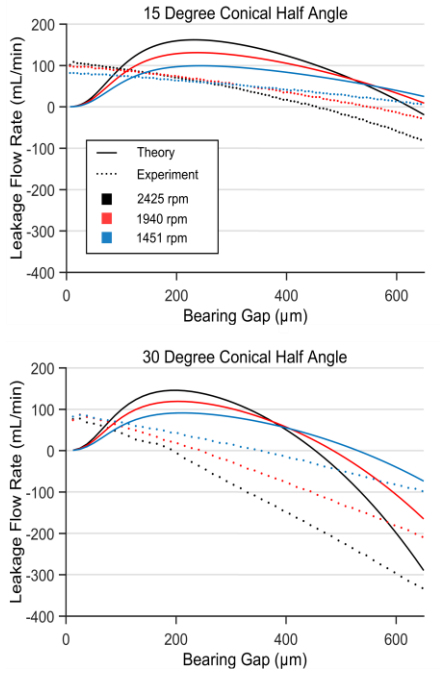

Figure 5. Flow curves comparing the narrow groove theory (NGT) and experimental data at different rotational speeds for 15° and 30° conical half angles. The NGT overestimates the bearing gap at which centrifugal forces alter viscous pumping trends, and small bearing gaps serve to enhance viscous pumping instead of choking flow.

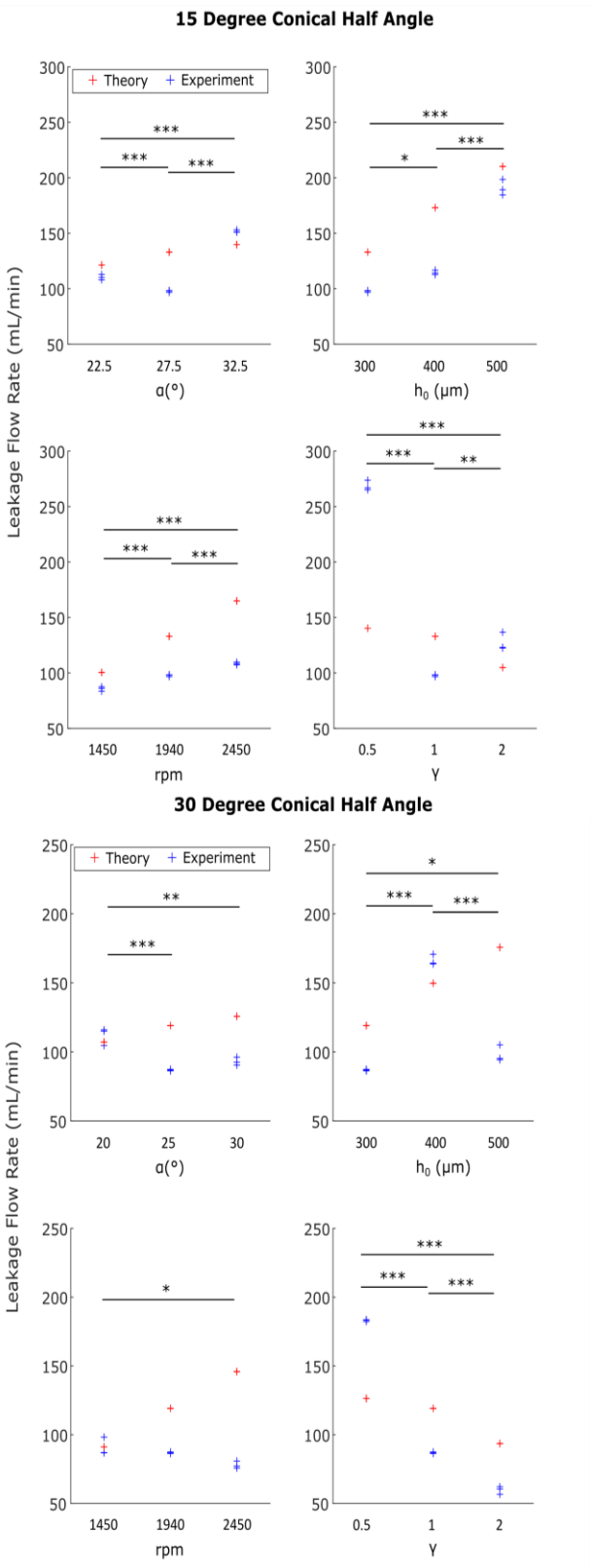

Figure 6. Leakage flow for each bearing design. Narrow groove theory only matches experiments in specific operating regions. Theory and experiments trend more closely in 15° bearings. Flow rate in 30° bearings varies less with changes in operating parameters, and they produce lower flow rates overall. than their 15° equivalents. ANOVA with post-hoc Tukey's HSD test was used for significance. *p< 0.05; **p<0.01; ***p<0.001

$$P^*(s) = P(s) - \frac{1}{2}\rho \sin(t)^4 \omega^2 s_1^2. \quad (11)$$

This correction predicts leakage flow more accurately than Chan et al.'s (8) over the tested bearing gap range for small conical half angles, and it approaches (8) as the half angle increases [19]. Results are shown in Fig. 4.

B. Validation of the Modified Analytical Model

The modified analytical model in Equation 11 was then used to predict leakage flow in the SGB at different rotational speeds, gaps, and conical half angles for comparison to experimental results. The analytical results were then compared with the experimental results accordingly. Fig. 5 demonstrates the relationship between bearing speed and flow rate with respect to the conical half angle.

For a 15° half angle, the modified analytical model correctly predicts that flow increases with speed but overestimates the magnitude. At 2425 rpm, NGT predicted +24% flow from baseline versus 11% measured; at 1450 rpm, NGT predicted a -25% flow, versus -12% measured. For a 30° conical half angle, flow decreased as speed increased (NGT: +23% at 2425 rpm, -24% at 1450 rpm; experimental: -10% at 2425 rpm, +4% at 1450 rpm). Theory was more accurate at lower bearing speed for both half angles (15% and 0.4% error for 1450 rpm; 34% and 47% error for 2425 rpm). Theory and experimental data trended similarly when flow was positive; however, theory predicted flow reversal at a larger gap than measured (NGT: +204 μm ±17 μm larger than experimental mean).

Although theory predicts flow independent of conical half angle, experiments demonstrated interaction between half angle and other bearing parameters. In the 15° half angle, there was a positive correlation between groove depth and flow rate but not in the 30° half angle. In the 15° half angle, a decrease in ridge-to-groove width ratio (1:1 vs 1:2) increased flow by 175% but only by 111% in a 30° bearing; whereas the NGT predicted a 5% increase in flow for both 15° and 30° bearings.

Flow sensitivity to geometry and operation was examined (Fig. 6). Theory suggests groove depth and rotational speed should impact flow most (groove depth: ±40% from baseline; speed: ±24%), but experiments indicate groove depth and ridge-to-groove width ratio impact flow most (groove depth: ±54% from baseline; ridge-to-groove width ratio ±87%). Flow correlated negatively with both half angle and ridge-to-groove width ratio (Pearson coefficients: -0.32, $p<0.05$, and -0.49, $p<0.001$, respectively). NGT also estimated the flow reversal gap; it overestimated the flow reversal gap for all designs but correctly predicted a negative relationship between rotational speed and reversal point and between ridge-to-groove width ratio and reversal point. Increasing the groove angle reduced the reversal gap, opposite of NGT prediction. Half angle had a negative correlation with reversal gap in both NGT and experiments (NGT: -0.92, $p<0.001$; experiment: 0.83, $p<0.001$).

IV. Discussion

In the past, NGT overestimated bearing load capacity and flow reversal bearing gap because it neglected inertia [2, 3, 19]. Although we found that accounting for inertia does not fully describe conical SGB gap flow behavior, we did identify correlation between flow reversal gap and conical half angle empirically and formulated an NGT correction term that captures half angle dependence. We also assessed NGT flow prediction with varied bearing geometry for RBP washout.

Discrepancies between the conical theory and NGT may occur because NGT includes an edge effect correction to compensate for undeveloped boundary layers at the spiral groove entrance, but conical theory does not. Since bearing eccentricity will invalidate the edge effect calculations, leading to overestimated pressure, flow, and force generation, we neglected edge effects in the conical NGT formulation.

Chan's correction improved NGT for flat SGB flow but not conical (Fig. 4), so we weighted it by the sine of the conical half angle squared to account for conical SGB. NGT is most accurate for flow in 15° (more cylindrical) half angle bearings, as indicated by the area between the experimental and theoretical curves. Experimental flow rates were highest at small half angles, suggesting better utility in an axial, rather than centrifugal, pump configuration. In all SGB geometries, NGT overestimates maximum flow gap and flow reversal gap. Thus, NGT only applies to washout at small conical half angles.

Although conical NGT predicts flow behavior independent of half angle, experiments suggest that flow behavior is dependent on half angle, particularly when inertial effects were dominant. Flow increased as groove depth increased from 400 to 500 μm in a 15° SGB (matched NGT), but decreased in a 30° SGB (mismatched NGT). We hypothesize this is because centrifugal forces are more closely aligned with the transverse length of the gap in the 30° SGB. Similar discrepancies between NGT and experiment flow were demonstrated by 1) increased flow in a 15° SGB as speed increases, but decreased flow in a 30° SGB with increased speed, and by 2) larger flow increase with increased groove width for a 15° bearing than a 30° bearing. We found NGT estimates flow most accurately at channel Reynolds numbers <1 and at rotational Reynolds numbers <3000, where viscous forces dominate flow behavior.

Past studies demonstrate significant half angle-dependence of centrifugal force on flow behavior in a conical annulus [21-23]. In these experiments, a rotating cylinder (0° half angle) forms a set of stable Taylor vortices with equal radii up to a Taylor number of 2500. A rotating cone, however, demonstrates a meridional cross flow that drives fluid near the rotating cone radially outward and fluid near the stationary wall inward. This meridional flow destabilizes Taylor vortices and causes spiraling Ekman-Couette rolls to form at lower Taylor numbers. The cross flow is apparent at half angles as small as 8 degrees and increases in magnitude as the half angle increases, until Taylor vortices are no longer formed at 45°. These studies demonstrate the significant half angle-dependent impact of centrifugal force on flow behavior in a conical annulus. The present work's half angle flow dependencies indicate the need for an analytical or empirical model that includes centrifugal and convective inertial effects for estimating SGB flow beyond the creep flow realm.

NGT is traditionally used to maximize SGB stiffness, necessitating small groove depths and bearing gaps (10-20 μm) [24]. SGBs designed for washout over stiffness in an RBP might require geometries that allow convective flow with larger grooves and bearing gaps (>30 μm) to avoid supraphysiological shear rates [6]. This study demonstrates that NGT cannot predict convective flow and that NGT approximates washout flow best for small half angle SGB geometries, which also had the largest pumping capacity. To accurately predict washout in an SGB, we recommend an empirical model in an operational area of interest. Further investigations will aim to develop an empirical model for conical SGB design.

V. Conclusion

This study evaluated the accuracy of an analytical model—the NGT—in predicting flow generated by conical SGB designs. When compared to experimental results, the NGT was insensitive to changes in the conical half angle, leading to the formulation of a novel inertia correction to improve NGT accuracy. The NGT is more accurate for small conical half angles because they favor creep flow conditions. Bearings with a smaller conical half angle generated larger flow rates and maintained viscous pumping capacity as both bearing and channel Reynolds numbers increased. Because of NGT's inability to predict interactions between groove geometry and the conical half angle, empirically derived models may be more useful in targeting a specific flow for a conical SGB design. We will focus on those models in future studies.

VI. Acknowledgement

The authors thank Rebecca Bartow, PhD, of the Department of Scientific Publications at the Texas Heart Institute, for her editorial contributions.

References

[1] E. A. Muijderman, "Spiral groove bearings," *Ind. Lubr. Tribol.,* vol. 17, no. 1, pp. 12-17, 1965.

[2] E. A. Muijderman, *Sprial groove bearings*, p.^pp. 169-170: Springer-Verlag, 1966.

[3] F. Amaral, S. Gross-Hardt, D. Timms, C. Egger, U. Steinseifer, and T. Schmitz-Rode, "The spiral groove bearing as a mechanism for enhancing the secondary flow in a centrifugal rotary blood pump," *Artif. Organs,* vol. 37, no. 10, pp. 866-74, Oct, 2013.

[4] T. Kink, and H. Reul, "Concept for a new hydrodynamic blood bearing for miniature blood pumps," *Artif. Organs,* vol. 28, no. 10, pp. 916-20, Oct, 2004.

[5] R. Kosaka, O. Maruyama, M. Nishida, T. Yada, S. Saito, S. Hirai, and T. Yamane, "Improvement of hemocompatibility in centrifugal blood pump with hydrodynamic bearings and semi-open impeller: in vitro evaluation," *Artif. Organs,* vol. 33, no. 10, pp. 798-804, Oct, 2009.

[6] R. Kosaka, M. Nishida, O. Maruyama, T. Yambe, K. Imachi, and T. Yamane, "Effect of a bearing gap on hemolytic property in a hydrodynamically levitated centrifugal blood pump with a semi-open impeller," *Biomed. Mater. Eng.,* vol. 23, no. 1-2, pp. 37-47, 2013.

[7] R. Paul, J. Apel, S. Klaus, F. Schugner, P. Schwindke, and H. Reul, "Shear stress related blood damage in laminar couette flow," *Artif. Organs,* vol. 27, no. 6, pp. 517-29, Jun, 2003.

[8] J. Sheriff, J. S. Soares, M. Xenos, J. Jesty, M. J. Slepian, and D. Bluestein, "Evaluation of shear-induced platelet activation models under constant and dynamic shear stress loading conditions relevant to devices," *Ann. Biomed. Eng.,* vol. 41, no. 6, pp. 1279-96, Jun, 2013.

[9] M. J. Simmonds, and H. J. Meiselman, "Prediction of the level and duration of shear stress exposure that induces subhemolytic damage to erythrocytes," *Biorheology,* vol. 53, no. 5-6, pp. 237-249, 2016.

[10] N. Watanabe, D. Sakota, K. Ohuchi, and S. Takatani, "Deformability of red blood cells and its relation to blood trauma in rotary blood pumps," *Artif. Organs,* vol. 31, no. 5, pp. 352-8, May, 2007.

[11] C. T. Esmon, "Basic mechanisms and pathogenesis of venous thrombosis," *Blood Rev.,* vol. 23, no. 5, pp. 225-9, Sep, 2009.

[12] D. J. Goldstein, R. John, C. Salerno, S. Silvestry, N. Moazami, D. Horstmanshof, R. Adamson, A. Boyle, M. Zucker, J. Rogers, S. Russell, J. Long, F. Pagani, and U. Jorde, "Algorithm for the diagnosis and management of suspected pump thrombus," *J. Heart Lung Transplant.,* vol. 32, no. 7, pp. 667-70, Jul, 2013.

[13] Y. Nose, "Design and development strategy for the rotary blood pump," *Artif. Organs,* vol. 22, no. 6, pp. 438-46, Jun, 1998.

[14] R. Virchow, 1856.

[15] F. Amaral, C. Egger, U. Steinseifer, and T. Schmitz-Rode, "Differences between blood and a Newtonian fluid on the performance of a hydrodynamic bearing for rotary blood pumps," *Artif. Organs,* vol. 37, no. 9, pp. 786-92, Sep, 2013.

[16] L. J. Leslie, L. J. Marshall, A. Devitt, A. Hilton, and G. D. Tansley, "Cell exclusion in couette flow: evaluation through flow visualization and mechanical forces," *Artif. Organs,* vol. 37, no. 3, pp. 267-75, Mar, 2013.

[17] T. Murashige, D. Sakota, R. Kosaka, M. Nishida, Y. Kawaguchi, T. Yamane, and O. Maruyama, "Plasma skimming in a spiral groove bearing of a centrifugal blood pump," *Artif. Organs,* vol. 40, no. 9, pp. 856-66, Sep, 2016.

[18] J. Bootsma, "Liquid-lubricated spiral-groove bearings," Mech, Mar. and Mat. Eng., TU Delft, Delft, Netherlands, 1975.

[19] W. K. Chan, K. T. Ooi, and Y. C. Loh, "Numerical and in vitro investigations of pressure rise in a new hydrodynamic blood bearing," *Artif. Organs,* vol. 31, no. 6, pp. 434-40, Jun, 2007.

[20] E. Szucs, "Fluid dynamics," *Similitude and modelling*, pp. 220-260, New York: Elsevier, 2012.

[21] M. Wimmer, "Transition from Taylor vortices to cross-flow instabilities," *Acta Mech.,* vol. 140, no. 1-2, pp. 17-30, 2000.

[22] N. P. Hoffmann, "Instabilities of shear flows between two coaxial differently rotating cones," *Phys. Fluids,* vol. 11, no. 6, pp. 1676-1678, 1999.

[23] M. N. Noui-Mehidi, N. Ohmura, and K. Kataoka, "Mechanism of mode selection for Taylor vortex flow between coaxial conical rotating cylinders," *J. Fluids Struct.,* vol. 16, no. 2, pp. 247-262, 2002/02/01/, 2002.

[24] H. Hashimoto, "Optimization of groove geometry for thrust air bearing to maximize bearing stiffness," *J. Tribol.,* vol. 130, no. 3, pp. 031101-031101, 2008.